

Linear Birefringence in Single-Mode Optical Fiber

M. MOHAMMED^{a,1}

^aDepartment of Physics, College of Science, Mustansiriyah University, Baghdad, Iraq

Abstract. The components of linear birefringence are essentially linear frequency dependence, Shape birefringence depends strongly on the frequency, for lower frequencies the value of B_c increases slowly with increasing v , is an approximately constant, and give maximum value (0.46) for frequencies within the region $1.8 < v < 2.2$. In contrast, when v increases at higher frequencies, the value of B_c steadily decreases. While it was shown that stress-related birefringence closely correlates with frequency, B_s has the same value as B_c and is (0.307) in the frequency value (5). This indicates that B_s contributes to B_c for large v values when the majority of the guided mode is contained inside the core. The minor axis of the core should align with the highest compressive stress, causing more power travel in the cladding and widening the mode size as the v value decreases. The fact that changes take place in that regime and that the cladding's stress-induced birefringence is the opposite of that of the core, that is, the main axis of the core elliptical experiences the greatest extent of the core compressive stress.

Keywords: Birefringence, Normalized frequency, non- circular core, lateral stress.

1. Introduction

Anisotropy in the refractive index distribution of the optical fiber core inevitably causes linear birefringence. In this scenario, the electrical permittivity of the core turns into a tensor, and the light's electric field vector components, which will cause the initial polarization state of the light change [1, 2]. There are two categories of processes that cause linear birefringence intrinsic and extrinsic. Intentional or unintentional effects originating from the production process, core shape, materials, etc. lead to the linear birefringence. Light propagates faster in a non- circular core if it is polarized in the direction of the lower core dimension. Through the photoelastic effect, the internal stress resulting from the differing thermal coefficients of the core materials (substrate and dopants) causes' linear birefringence [3].

Recently, there are many researches that dealt with the subject of birefringence in a fiber, for example, a technique was used to measure the spatial distribution of birefringence in single-mode optical fibers, depending on the optical time-domain reflectometer of an experimentally used linear rotating polarizer. M. Wuilpart, et al. [4]. A technique was used to measure the phase and group birefringence of an optical fiber. And that is based on several measurements of the differential group delay of the twisted fibers and then calculating the value of the birefringence in the fiber. M. Legre,

¹ M. MOHAMMED, Corresponding author, Department of Physics, College of Science, Mustansiriyah University, Baghdad, Iraq; E-mail: dr.miamiph@uomustansiriyah.edu.iq.

et al. [5]. The lateral stress effect that happens in the optical fiber when the fiber is exposed to considerable bending causes birefringence in the fiber is bent severely via the cross section. U.L. Block, et al. [6]. In an experimental investigation, the length of the optical fiber in use was altered, and the impact on the single-mode fiber's usual refraction was evaluated. M. Mohamed [7]. The link between the fiber core's ellipticity and the residual stress imposed by a change in ellipticity, which causes model birefringence in single-mode optical fiber, was examined. M.A. Mohamed, et al. [8]. It was also investigated how altering a single-mode fiber's curvature radius affected measurements of increased refraction as a result of decreasing the fiber's radius. M. Mohamed [9]: By leveraging compressible microfiber gratings (MFBGs) and impact rapid field transient on the mode coupling, strong birefringence in photonic crystal fibers was theoretically achieved. A. Kudlinski, et al. [10]: An optical fiber current sensor (OFCS) based on the Faraday magnetic effect was used to yield linear birefringence. R. Wang, et al. [11]. The method of elements was used to direct the light along a liquid core of fiber using an open V groove, in this way they are able to achieve high birefringence in single-mode fiber, and then it is able to obtain polarimetric liquid sensing. Tavakol Nazar, et al. [12]. Study single-mode fiber birefringence measurement utilizing polarimetric fiber ring laser probed through beat frequency, splitting of fiber modes into orthogonal polarization modes owing of the normal birefringence of the fiber in the ring laser. This causes two different beat frequencies to be created simultaneously: one is the longitudinal mode beat frequency, while the other is the polarization mode beat frequency. So we will get two expressions for the birefringence change of the fiber in a longitudinal arrangement, and the polarization mode is superior to the frequency signals, which is very convenient for users for the measurement of birefringence in a short-length single-mode fiber. X. Yu, et al. [13]. An analysis using numerical simulation of the transverse mechanical stress induced by model birefringence in a single-mode optical fiber in a Long Period Grating Fibre Sensor (LPGFS), by adding LPGFS to a smart composite material's polymer matrix. This study may be useful for its application in different fields such as aviation, industry and medicine. S. Miclos, et al. [14]. A new method for assessing residual birefringence in single-mode optical fibres, where the polarimetric is based on the use of Muller and Poincaré calculation, this method is considered simple, accurate and also non-destructive, as it allows us to measure the azimuth and elliptic angles of the spontaneous mode of polarization in a single-mode fiber. A. Rojas-Sanchez, et al.[15]. The polarization evolutions for both the continuous wave and the pulse profile are investigated by the changing that occurs in ellipticity and ellipse rotation, which caused the linear and non-linear birefringence in optical fiber, using numerical simulation to analyze the continuous wave and ultrashort pulse using the twisted single-mode optical fiber. H. E. Ibarra-Villalon, et al. [16]. In a practical study to measure model birefringence in optical fibers when the core of the fiber is elliptical and using very low elliptically, the results show that model birefringence is strongly frequency dependent, especially when the fiber is run at a normalized frequency near the higher cut-off mode region. M. A. Mohammed [17].

Our approach to determining liner in single-mode optical fibers was described in this study, along with an explanation of the causes of birefringence in fibers, including whether it results from manufacturing process or external influences ton optical fiber. The following is how the research study is structured: Includes in Section 1 is the theoretical part, where we discuss the mechanisms underlying birefringence degeneration and how it manifests in fibers. Then what other elements result in

birefringence degeneration in optical fibers, which include manufacturing techniques that create fibers from a non-nucleus circular core or elasto-optic index alterations that generate asymmetric lateral stress. While Section 2 deals with the practical part and the system of work and Section 3 provides a review of the most significant experimental findings. While the results we got from our research are described in Section 4.

2. Theoretical Part

2.1. Birefringence Mechanisms

When the ideal fiber's circular symmetry is disrupted, an anisotropic distribution of the refractive indices develops in the core area, which is known as birefringence. Fiber asymmetry is caused either geometrical distortion of the fiber core or anisotropy in the material properties, manifested as variations in the elasto-optic, magneto-optic, or electro-optic index. Figure (1) depicts the basic mechanics of birefringence. The fiber's internal birefringence is added during the fiber manufacture process. Most majority produce result in linear birefringence with linearly polarized modes [18].

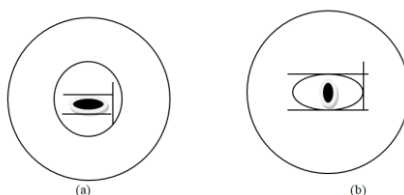


Figure 1. Single – mode fibers experience birefringence as a result of (a) a non- circular core and (b) an asymmetrical lateral stress [2].

2.2. Non- circular Core

The geometrical anisotropy of the non - circular core causes linear birefringence in the fibers. Light travels fastest when polarized along the direction of polarization minimum, which is the smallest transverse dimension of the core. This is the fast axis of the birefringence. In certain core configurations, birefringence depends strongly on the frequency, or value of V , at which the fiber is to be run. If the frequencies are only close to the higher mode cutoff frequency, the birefringence of the small- core fiber ellipticity can be approximated to ($e^2 \ll 1, \Delta \ll 1$) by [19, 20]:

$$B_c = \frac{e^2 (2\Delta)^{3/2}}{a} \cdot \frac{3\pi^2 \nu^2}{(\nu + 2)^4} \quad (1)$$

This birefringence B_c is essentially constant, and the maximum frequencies are corresponding to the region $1.8 < \nu < 2.2$, fiber run normally. From equation ($e^2 = 1 - b^2 / a^2$), where $b = 2.29$ and $a = 2.5$ are the semi- minor and major axes of the core, and ($\Delta = 2.3 \times 10^{-3}$) is the relative index difference between core and cladding. The fast axis of this birefringence is in the direction of the minimum polarization limit of the core, i.e., it is parallel to the minor axis of the ellipse.

2.3. Asymmetrical Lateral Stress

Any transverse asymmetrical causes linear birefringence in fiber via changes in the elastooptic index. Because the thermal contraction of the doped non-circularly symmetric regions of the fiber varies, stress may be internally frozen into the fiber during fabrication. In a homogeneous, weakly guiding elastic single-mode fiber, the birefringence caused by transverse stress has a typical form [21, 22]:

$$B_s = 2\pi n^3 |P_{44}| (1 + N) \left(\frac{\sigma}{E}\right) \nu \quad (2)$$

Equation (2) uses $n=1.46$ as the refractive index of the fiber's material regardless of whether the stress is internal due to differential thermal expansion or external owing to lateral pressure on the fiber. $E=7.3 \times 10^{10} \text{ N/m}^2$ stand in for the Young's modulus, $N=0.17$ for the Poisson's ratio, and $P_{44} = -0.075$ for the strain-elastooptic tensor component. Comparatively $\sigma = 4.6 \times 10^5 \text{ N/m}^2$ denote the transverse stress anisotropy in the core, which indicates the difference between the highest and minimal stress components [23, 24]. Because the fast axis of stress birefringence in silica fibers ($P_{44} < 0$) and the direction of the highest both point in the same direction, the stress birefringence is linear.

Weak frequency dependences of n and P_{44} in Equation (2) may be disregarded for silica and fibers as well as for the very small spectral ranges of relevance here. we may choose to ignore the consequence, which is that stress related birefringence has been demonstrated to be directly proportional to frequency ν . Then, using this proportionality, it is feasible to differentiate between the stress birefringence and the birefringence resulting from core ellipticity, which has been demonstrated to be a separate component of ν

3. Experimental Parts

Given that the fiber single – mode and has a core diameter of ($2a = 5 \mu\text{m}$), small core ellipticity ($e^2 = 0.161$), and an index different between the core and cladding of ($\Delta = 2.3 \times 10^{-3}$), we may state the following. Figure (2) depicts a fiber that has been used in an experimental to simulate birefringence. In order to the Linear polarized light state from the He-Ne laser operating at (632.8 nm) onto a modified Fresnel rhombus until we convert the linear to a circular one, we first centered the Linearly polarized light from the He-Ne laser operating at (632.8 nm) onto a modified Fresnel rhombus. Afterward, we direct the circularly polarized light onto the polarizer in order to identify the polarization plane of the newly emerged linearly polarized beam. The light is coupled to a plane of polarization defined by the fiber through a microscope objective. A microscope objective is then used to focus the light that emerges from the optical fiber's end onto the analyzer. We install a PIN-SI image detector with a low-noise pre-amplifier after the light beam enters the detecting system. A lock-in amplifier that uses the optical chopper signal as its reference feeds the output electric signal from the detecting system [1, 25]. Fibers with the characteristics listed in table 1 were utilized. By etching the fiber end in hydrofluoric acid and confirming the deformation at the end of the optical fiber using a high – powered optical microscope, the deviation from circularity was identified. This experimental approach intends to identify the linear birefringence to acquire the polarization state of the light beam arising for a certain

polarization plane of the coupled light beam. The polarizer is rotated (45°) with respect to the principle axes of the fiber to create the polarization plane, ensuring that the two electric field components are equally excited for a prolonged period of time from these axes. The planes of polarization in which the linear polarization state of the propagation beam is kept are the major axes of an optical fiber. By altering the polarizer and checking the resulting beam's polarization state using the analyzer, these fiber axes may be identified [26, 27].

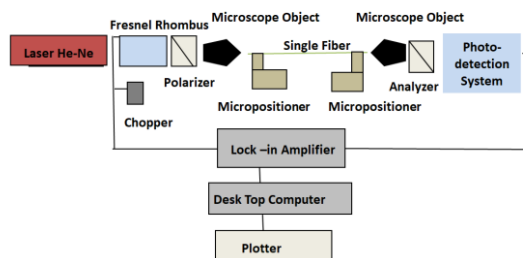


Figure 2. A fiber's birefringence arrangement [19].

Table 1. Birefringence resulting from the elliptical core and stress changes as a function of normalized frequency at $e^2 = 0.161$, $\Delta = 2.3 \times 10^{-3}$ and $a = 2.5 \mu m$.

V	B_c	B_s
0	0	0
0.2	0.05	0.0123
0.4	0.142	0.025
0.6	0.233	0.041
0.8	0.307	0.05
1	0.365	0.062
1.2	0.406	0.072
1.4	0.433	0.086
1.6	0.45	0.098
1.8	0.459	0.11
2	0.462	0.12
2.2	0.46	0.13
2.4	0.454	0.145
2.6	0.446	0.16
2.8	0.436	0.173
3	0.425	0.185
3.2	0.414	0.198
3.4	0.402	0.21
3.6	0.389	0.22
3.8	0.377	0.23
4	0.365	0.24
4.2	0.352	0.25
4.4	0.341	0.26
4.6	0.329	0.28
4.8	0.318	0.29

5	0.307	0.307
5.2	0.297	0.321
5.4	0.287	0.334
5.6	0.278	0.346
5.8	0.268	0.359
6	0.259	0.371

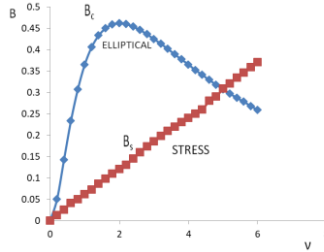


Figure 3. Birefringence resulting from the elliptical core and stress changes as a function of normalized frequency at $e^2 = 0.161$, and $\Delta = 2.3 \times 10^{-3}$ and $a = 2.5 \mu\text{m}$.

4. Results and Discussion

Fiber optical is used in this research has internal model birefringence introduce during the manufacturing fiber result in either a geometrical deformation of a noncircular core shape (B_c) in some regions of the fiber core or a symmetrical lateral stress (B_s) result in differing coefficients of thermal expansion between cladding - core region, each of these factors occur a linear birefringence in the fiber. Was calculated shape birefringence from the equation (1) for small-core ellipticity ($e^2 = 0.161$ and $\Delta = 2.3 \times 10^{-3}$). Figure 3 shows us the shape birefringence changes arising from a change in the normalized frequency v . Lower frequencies see a gradual increase in the value of B_c , which is roughly consistent and reaches a maximum value of (0.46) in typical operating range of frequencies ($1.8 < v < 2.2$). Whereas For higher frequencies value, B_c decreases slowly with increasing v . The stress birefringence has also been determined using equation (2), and figure 3 illustrates it as a function of normalized frequency v . The stress birefringence grows linearly with increasing v . While keeping in mind that when the normalized frequency value is (5), as shown in Figure (3), the value of B_s takes the same value as B_c , which is to be (0.307). In other words, the B_s value is additive to the B_c value for large v values falls, thanks to an expanding mode size. Because the opposite of signal produced in the core region by the birefringence caused by the stress in the cladding, signal changes in the region may be explained. As a result, we observe that the core ellipse's principle axis is the one that experiences the most compressive stress.

5. Conclusion

The elliptical core deformation and the stress anisotropy introduce during the fiber's fabrication are the main caused of birefringence in optical fiber. The frequency dependence of the linear birefringence components BC and BS are nearly linear. Shape

birefringence is mainly high and almost constant in the range of frequencies $1.8 < V < 2$, where the fiber is in a typical working state normally. Shape birefringence is substantially frequency dependent. It was discovered that stress-induced birefringence is directly related to frequency. The fast axis of this birefringence is parallel to the minor axis of the ellipse and points in the direction of the core's lowest polarization.

References

- [1] Vieria AJV and Siliva MTC. *J. Electrical and Computer Engineer.* 1988; 3: 57- 62 (1988).
- [2] Agrawal GP. *Nonlinear Fiber Optics (3rd Edition).* Elsevier, 2006.
- [3] Chowdhury D and Wilcox D. *Quant. Electronic.* 2000; 6: 227-232 (2000).
- [4] Wuilpart M, Megret P, Blondel M, Rogers AJ, Defosse Y. *IEEE Photo. Techn. Letters.* 2002; 13: 836-838.
- [5] Legre M, Wegmuller M and Gisin N. *J. Lightwave Technology.* 2003; 21: 3374.
- [6] Block UL, Dignonnet MJF, FejerDangui MM. *J. Lightwave Technology.* 2006; 24: 3374.
- [7] Mohamed M. *Journal of College of Science, Al- Mustansiriyah University, Baghdad, Iraq.* 2010; 21: 20-27.
- [8] AL-Dulaimy AA, Mohamed MA. *J. College of Education, Al- Mustansiriyah University, Baghdad, Iraq.* 2011; 3: 247-261.
- [9] Mohamed M. *J. College of Education, Al- Mustansiriyah University, Baghdad, Iraq.* 2011; 3: 85-98.
- [10] Kudlinski A, Bendahmane A, Labat D, Virally S, Murray RT, Kelleher EJR and Mussot A. *J. Optics Express.* 2013; 21: 8437-8443.
- [11] Wang R, Xu S, Li W and Wang X. *J. Opti. and Quant. Electronics.* 2016; 48: 3374.
- [12] Joo NB, Hwang JH, Paulson B, Park J, Jhon YM and OH K. *J. Opti. Express.* 2017; 25: 24714-24726.
- [13] Yu X, Chen X, Zhang J, Gao Y and Liu S. *J. of Light wave Technology.* 2018; 36: 2204-2210.
- [14] Miclos S and Lancranjan II. *J. Composite Structures.* 2019; 216: 15-26.
- [15] Sanchez AR and Tentori D. *OSA Continuum.* 2020; 3: 1650-1656.
- [16] Ibarra-Villalon HW, Pottiez O, Gómez-Vieyra A, Lauterio-Cruz JP and Bracamontes-Rodriguez YE. *J. Optics.* 2021; 23: 123501.
- [17] Mohammed MA. *Ibn Al Haitham Journal for Pure and Applied Science.* 2022;1: 39-49.
- [18] Rashleigh SC. *Light Wave Technology.* 1983; 1: 312-330.
- [19] Eickhoff W, Yen Y and Ulrich R. *J. Appl. Optics.* 1981; 20: 3428-3435.
- [20] Summat RA. *J. Electr. Letter.* 1980; 16: 615-616.
- [21] Alam MS and Anwar SRM. *J. Electrical and Computer Engineer.* 2010; 5: 257-261.
- [22] Park Y, Paek UC and Kim Y. *J. Opti. Letter.* 2002; 2: 1291-1293.
- [23] Islam MM and Zahid MA. *J. Electri. Engineering.* 2009; 36: 10-15.
- [24] Dianov EM and Mashinsky VM. *J. Light Wave Technology.* 2005; 23: 3500–3508.
- [25] Marcuse D. *Theory of Dielectric Optical Waveguide.* Academic Press, New York, 1991.
- [26] Shen DS. *J. Light Wave Technology.* 2007; 25: 2700-27050.
- [27] Rashleigh SC. *J. Opti. Letter.* 1982; 7: 294–296.